



THE UNIVERSITY *of* EDINBURGH

Edinburgh Research Explorer

## Effect of pH and pressure on uranium removal from drinking water using NF/RO membranes

### Citation for published version:

Schulte-Herbruggen, H, Correia Semiao, A, Chaurand, P & Graham, M 2016, 'Effect of pH and pressure on uranium removal from drinking water using NF/RO membranes', *Environmental Science and Technology*, vol. 50, no. 11, pp. 5817–5824. <https://doi.org/10.1021/acs.est.5b05930>

### Digital Object Identifier (DOI):

[10.1021/acs.est.5b05930](https://doi.org/10.1021/acs.est.5b05930)

### Link:

[Link to publication record in Edinburgh Research Explorer](#)

### Document Version:

Peer reviewed version

### Published In:

Environmental Science and Technology

### General rights

Copyright for the publications made accessible via the Edinburgh Research Explorer is retained by the author(s) and / or other copyright owners and it is a condition of accessing these publications that users recognise and abide by the legal requirements associated with these rights.

### Take down policy

The University of Edinburgh has made every reasonable effort to ensure that Edinburgh Research Explorer content complies with UK legislation. If you believe that the public display of this file breaches copyright please contact [openaccess@ed.ac.uk](mailto:openaccess@ed.ac.uk) providing details, and we will remove access to the work immediately and investigate your claim.

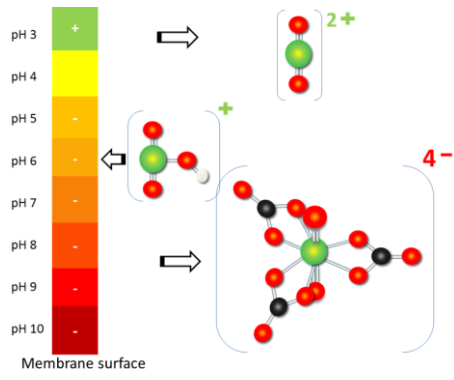




17 ABSTRACT ART

18

19



20 **Abstract.** Groundwater is becoming an increasingly important drinking water source.  
21 However, the use of groundwater for potable purposes can lead to chronic human  
22 exposure to geogenic contaminants, *e.g.* uranium. Nanofiltration (NF) and reverse  
23 osmosis (RO) processes are used for drinking water purification, and it is important to  
24 understand how contaminants interact with membranes since accumulation of  
25 contaminants to the membrane surface can lead to fouling, performance decline and  
26 possible breakthrough of contaminants. During the current study laboratory  
27 experiments were conducted using NF (TFC-SR2) and RO (BW30) membranes to  
28 establish the behaviour of uranium across pH (3-10) and pressure (5-15 bar) ranges.  
29 The results showed that important determinants of uranium-membrane sorption  
30 interactions were (i) the uranium speciation (uranium species valence and size in  
31 relation to membrane surface charge and pore size) and (ii) concentration polarisation,  
32 depending on the pH values. The results show that it is important to monitor sorption  
33 of uranium to membranes, which is controlled by pH and concentration polarisation,  
34 and, if necessary, adjust those parameters controlling uranium sorption.

35

36 **Key words:** sorption, concentration polarisation, nanofiltration, reverse osmosis,  
37 speciation, uranium

38

39

40

41 **Introduction.** Groundwater is an increasingly important source of drinking water,<sup>1</sup>  
42 especially for developing nations in *e.g.* Africa<sup>2</sup> but also in European countries, where  
43 20-100% of drinking water is sourced from groundwater.<sup>3</sup> As a consequence of  
44 hydrological and geochemical processes uranium is naturally present in groundwater  
45 at concentrations from below detection to hundreds of  $\mu\text{g L}^{-1}$ .<sup>4-6</sup> Indirect release of  
46 uranium into water may also occur through *e.g.* phosphate ore processing, phosphate  
47 fertilizer use, gold and tin-mining.<sup>7-10</sup> Uranium is above all chemically toxic, and  
48 although chronic exposure to uranium is not well understood,<sup>11-14</sup> studies have  
49 identified kidney, bone, liver, heart and brain as potential targets following exposure  
50 through ingestion of uranium-containing water.<sup>11,15-18</sup> The maximum acceptable  
51 concentrations (MAC) for uranium vary between public authorities, *e.g.* Canada uses  
52 an interim MAC of  $20 \mu\text{g L}^{-1}$ , whilst the US has adopted the same limit as the WHO  
53 provisional drinking water limit of  $30 \mu\text{g L}^{-1}$ .<sup>19</sup> However, concentrations as low as 2  
54  $\mu\text{g/L}$  may be hazardous for infants.<sup>20</sup> Membrane technology such as nanofiltration  
55 (NF) and reverse osmosis (RO) are frequently used for drinking water purification<sup>21-24</sup>  
56 since they efficiently remove a wide range of contaminants, including uranium.<sup>25</sup>  
57 Membrane technology is also being considered for application in remote sites due to  
58 the modular and flexible configuration and, if coupled with renewable energy, their  
59 independence from intermittent or absent energy supplies.<sup>26-28</sup> The performance of a  
60 membrane system using ultrafiltration, NF or RO membranes, coupled with a  
61 renewable energy supply was tested in the field. The results showed that although the  
62 system performed well in terms of producing permeate with low concentrations of  
63 most analytes *e.g.*  $\text{Ca}^{2+}$ ,  $\text{Mg}^{2+}$ ,  $\text{Mn}^{2+}$ ,  $\text{SO}_4^{2-}$ ,  $\text{Na}^+$  and  $\text{Cl}^-$ , the behaviour of uranium in  
64 the system differed from that of most other inorganic species found in the water.

65 Moreover, uranium strongly interacted with the membranes.<sup>29</sup> It was deduced that this  
66 was largely due to the complex chemical behaviour of uranium, since its speciation  
67 varies widely depending on physico-chemical parameters such as available inorganic  
68 or organic ligands and pH of the water.<sup>29-32</sup> For instance, the presence of calcium  
69 affects uranium speciation and is likely to affect uranium interaction with the  
70 membranes.<sup>29</sup> A variety of processes can be responsible for the observed uranium  
71 uptake, including precipitation of uranium to the membrane, physi-sorption (such as  
72 hydrogen bonding or electrostatic attraction) or chemi-sorption resulting in bond  
73 formation between uranium and membrane functional groups. Before the exact  
74 mechanisms are determined, the more general terms “sorption” or “uranium-  
75 membrane interaction” will be used in this paper. To establish the processes involved  
76 in the interaction of uranium with the membrane, controlled laboratory experiments  
77 are needed, isolating one factor at a time: individual membranes, solution  
78 composition, pH and pressure ranges. The present study focused on uranium in the  
79 absence of other major ions, *e.g.* calcium, in order to determine the membrane  
80 interactions due to uranium alone. Although there have been studies investigating  
81 uranium retention using NF and RO<sup>33-36</sup> none have investigated the specific  
82 interactions between membranes and uranium during the water purification process.  
83 Therefore, the aims of this study were to determine (i) the effect of pH and speciation  
84 on uranium-membrane interactions by NF and RO membranes; (ii) the effect of  
85 membrane pore size and (iii) the effect of pressure on the uranium-membrane  
86 interactions.

87

88 **Materials and Methods.** The behaviour of uranium was investigated using an  
89 experimental feed solution containing 0.5 mg L<sup>-1</sup> uranium (uranyl nitrate, TAAB,  
90 UK), background electrolyte and buffer (20 mM NaCl and 1 mM NaHCO<sub>3</sub>, Fisher  
91 Scientific, UK). The uranium concentration chosen is comparable to concentrations  
92 found naturally.<sup>4,29,37,38</sup> MilliQ water was used to prepare all solutions (Elga Purelab  
93 Ultra, High Wycombe, UK). The pH of the experimental solution was adjusted (1 M  
94 HNO<sub>3</sub>, VWR Aristar, or 1 M NaOH, Fisher Scientific) according to the conditions to  
95 be tested (described later), prior to adding the solution to the stainless steel cross-flow  
96 system (MMS, Switzerland). Two membranes with different molecular-weight cut-off  
97 (MWCO) values but of similar materials (polyamide active layer on a polysulphone  
98 support layer) were selected: TRC-SR2, a NF membrane (Koch Membrane systems,  
99 USA) and BW30, a RO membrane (Dow Filmtec). Cross-flow experiments were  
100 carried out with and without applied pressure to investigate the effects of pressure on  
101 uranium-membrane interactions. Two types of cross-flow experiments were  
102 conducted: 1) across the pH range 3-10 (in units of one, with one pH value per  
103 experiment) but with *no* applied pressure and 2) at two selected pH values (pH 6 and  
104 8.5), across the pressure range 5-15 bar (in steps of 2.5 bar, one pressure and pH value  
105 per experiment).

106

107 **Filtration set-up and procedure.** New rectangular membrane coupons (membrane  
108 area of 0.0046 m<sup>2</sup>) were cut for each experiment from a membrane sheet. The  
109 coupons were washed and soaked in MilliQ water at 4°C overnight, washed again,  
110 before being mounted in the stainless steel cross-flow system, operated in total  
111 recirculation mode. Membranes were compacted using MilliQ water at 25 bar prior to

112 experiments and a solution sample was collected as a quality check. A detailed  
 113 description of the experimental set-up is given in the supporting information (SI) and  
 114 a schematic is published in Semião and Schäfer.<sup>39</sup> The system was drained and  
 115 experimental solution added (feed volume of 2 L). The flow-rate was set to 0.6 L min<sup>-1</sup>  
 116 and, for *pressure experiments*, pressure was applied at this point. Temperature,  
 117 pressure, feed flow, feed and permeate pH and conductivity were monitored  
 118 throughout the experiments which lasted up to seven hours. Feed and permeate  
 119 samples were regularly collected. The pH value of the feed solution was adjusted (1  
 120 M HNO<sub>3</sub>, VWR Aristar, or 1 M NaOH) during experiments to maintain the pH value  
 121 within ± 0.2. The pH value of permeate samples deviated from that of the feed with  
 122 up to a value of ± 0.5.

123

124 The mass of uranium sorbed by the membrane (mg U m<sup>-2</sup> of membrane) was simply  
 125 calculated as the mass uptake of uranium by the membrane divided by the membrane  
 126 area. To report the mass sorbed as percentage uptake, the uranium mass sorbed by the  
 127 membrane was calculated in relation to the initial mass of uranium available in the  
 128 feed (*i.e.* 1 mg U):

129

$$Uptake(\%) = \frac{V_{b0}C_{b0} - V_{bf}C_{bf} - \sum_{i=0}^{i=n} V_S C_{si}}{V_{b0}C_{b0}} \times 100 \quad \text{Eq. 1}$$

133



134 where,  $V$  = volume (L),  $C$  = uranium concentration ( $\text{mg L}^{-1}$ ),  $s$  = permeate or feed  
135 sample taken,  $b$  = bulk (or feed),  $f$  = final,  $0$  = initial and  $n$  indicates the number of  
136 samples collected during the experiment.

137

138 Following completion of each experiment and the removal of the membrane, the  
139 system was thoroughly washed using dilute  $\text{HNO}_3$  (2%, v/v Analar, VWR) followed  
140 by consecutive washes with MilliQ water. For quality control purposes a sample was  
141 collected of the final system washes and analysed for uranium content (below  
142 detection in washes).

143

144 **Chemical analysis and quality control.** The uranium concentrations in the feed  
145 samples was determined by Inductively Coupled Plasma – Optical Emission  
146 Spectroscopy (ICP-OES, Optima 5300 DV, Perkin Elmer, USA) whilst those in the  
147 permeate samples were determined by Inductively Coupled Plasma – Mass  
148 Spectrometry (ICP-MS, Agilent 7500ce). Calibration standards were prepared using a  
149 uranium stock solution ( $1000 \text{ mg L}^{-1} \text{ U}$ , Merck) and dilute  $\text{HNO}_3$  (2% v/v, Aristar,  
150 VWR International, UK). For both ICP-OES and ICP-MS analysis, check standards  
151 and blank samples (2% v/v  $\text{HNO}_3$ ) were inserted after every 5-10 samples during the  
152 run. The accuracy of the calibration was asserted for both techniques by analyzing a  
153 standard reference solution (ICP Multi Element Standards Solution VI, Certipur). The  
154 average value obtained for the standard reference material during ICP-OES analysis  
155 was  $0.978 \pm 0.140 \text{ mg L}^{-1}$  (expected:  $1.0 \pm 0.05 \text{ mg L}^{-1}$ ). The average value for the  
156 ICP-MS analysis was  $0.979 \pm 0.59 \mu\text{g L}^{-1}$  (expected:  $1.0 \pm 0.05 \mu\text{g L}^{-1}$ ).

157

158 **Micro-X-ray Fluorescence spectroscopy.** The penetration of uranium into  
159 membranes was explored for selected experiments using micro-X-ray Fluorescence  
160 spectroscopy ( $\mu$ -XRF, XGT-7000 microscope from Horiba Jobin Yvon). Cross-  
161 sections of the dry membranes were cut using scissors and placed between paperboard  
162 support for analysis in a line over multiple points (1000s/point) along the membrane  
163 cross-section with an incident X-ray beam size of 10  $\mu$ m (Rh target, accelerating  
164 voltage of 50 kV, current 1 mA). More detailed information on this method is  
165 provided in the Supporting Information.

166

167 **Speciation modeling.** The modeling of the uranium and other ions present in the  
168 aqueous solution was carried out across the pH range 3-10 using visual Minteq 2.53  
169 (KTH, Stockholm, Sweden), as described in Rossiter et al.<sup>29</sup>

170

171 **Membrane characterization.** NF and RO membranes have been shown by other  
172 studies to have different surface chemistries. The BW30 membrane consists of a fully  
173 aromatic polyamide active layer coated with an aliphatic layer rich in alcoholic  
174 groups, whilst other membranes have a fully or semi aromatic polyamide active layer  
175 with no coating.<sup>40</sup> As these different functional groups may affect membrane surface  
176 charge<sup>41</sup> and hence potentially, the interaction with different uranium species, the  
177 membrane zeta potential was measured in background electrolyte solution (1 mM  
178 NaHCO<sub>3</sub> and 20 mM NaCl) using an electro-kinetic analyzer (EKA, Anton Paar,  
179 Austria). MWCO and pore-size was determined experimentally using a range of  
180 neutral organic molecules (dioxane, dextrose (Fisher, UK), xylose (Acros Organics,  
181 UK) and polyethylene glycol of different molecular weight (400, 600 and 1000 g mol<sup>-1</sup>

182 <sup>1</sup>, Fisher, UK)) at a concentration of 25 mg carbon L<sup>-1</sup> applied to the same membrane  
183 sample, following methods described in Hilal et al. and Nghiem et al.<sup>42,43</sup> For the  
184 determination of pore radius, film theory was used<sup>44</sup> and a correlation was used to  
185 estimate the mass transfer coefficient of UO<sub>2</sub><sup>2+</sup>.<sup>45,46</sup> Organic carbon concentrations  
186 were measured in non-purgeable organic carbon mode using a TOC Analyser  
187 (Shimadzu TOC-VCPH, UK) with an ASI autosampler and high-sensitivity catalyst.  
188 Salt flux was calculated using conductivity measurements. Average permeability and  
189 standard deviation of the membrane coupons was calculated using the stabilized flux  
190 measurements during compaction.

191

## 192 **Results and Discussion.**

193 **Membrane characterisation.** The zeta potential measurements showed that the net  
194 charge of TFC-SR2 and BW30 were similar to each other and varied with pH: the  
195 overall charge was positive at pH 3, the iso-electric points for TFC-SR2 and BW30  
196 were at pH 4.25 and pH 4.19 (Table 1), respectively, after which the magnitude of the  
197 negative charge increased with increasing pH value. The nominal MWCO (90%  
198 retention), permeability measurements and pore radius calculation showed that TFC-  
199 SR2 has a more open structure compared with BW30 (Table 1).

200

201 **Uranium sorption to NF and RO membrane across the pH range 3-10.** The  
202 objective of these experiments was to determine the influence of pH on the extent of  
203 uranium sorption by the membrane without the application of pressure. The results for  
204 uranium sorption by the membrane are shown in Figure 1 together with the dominant  
205 uranium species across the pH range. Sorption increased from < 5.5% at pH 3 for both

206 membranes, to a maximum of 31% for BW30 and 50% for TFC-SR2 at pH 6.  
207 Thereafter sorption decreased to < 10% at pH 10 for both membranes. Notably, the  
208 sorption was similar for both membranes at the pH extremes, whereas, although  
209 following the same pattern, the sorption was at least 20% lower for BW30 at peak  
210 sorption than for TFC-SR2.

211

212 The results of these experiments confirm the observations by Rossiter et al.<sup>29</sup> that  
213 there is a strong interaction between uranium and NF/RO membranes, especially at  
214 pH values 5-7. The speciation modelling showed that the dominant uranium species  
215 vary greatly with pH and the valence of the uranium species also changed from being  
216 positive at acidic pH (pH 3-6), to either neutral or carrying single negative charge  
217 under near-neutral conditions to highly negative at alkaline pH (pH 8-10). Since the  
218 overall membrane charge also varies with pH, going from weakly positive (pH 2-4) to  
219 highly negative at pH values above pH 5, charge interactions are likely to play an  
220 important role in uranium sorption. Electrostatic repulsion can explain the low  
221 interaction between uranium and the membranes at pH 3-4 and pH 8-10, where  
222 uranium species and membrane carry the same charge. Electrostatic attraction is a  
223 likely contributor to the greater sorption of uranium to the membrane at pH 5 and 6,  
224 which was 49% for the TFC-SR2 and varied from 25 to 31% for the BW30  
225 membrane. Charge interactions between uranium species and NF/RO membranes  
226 hence govern uranium sorption to the membranes.

227

228 The uranium species also vary in molecular weight (Table 2), and hence size  
229 exclusion might contribute to the difference in sorption for both membranes studied.

230 At pH 5-6, where high uranium sorption takes place, the MW of the main uranium  
231 species ( $\text{UO}_2\text{OH}^+$ ,  $\text{UO}_2^{2+}$  and  $\text{UO}_2\text{CO}_3$ , Figure 1) is considerably lower (270-330 g  
232  $\text{mol}^{-1}$ ) than the MWCO of the TFC-SR2 membrane (MWCO: 486 g  $\text{mol}^{-1}$ ). The size  
233 difference between the membrane MWCO and the uranium species, allied to charge  
234 attraction between the negatively charged membrane and the positively charged or  
235 neutral uranium species, suggests ease in penetrating the TFC-SR2 membrane<sup>47</sup> in the  
236 absence of pressure and with access to the active and support layers for sorption.  
237 Charge attraction will also occur between the uranium species and the BW30  
238 membrane, as both TFC-SR2 and BW30 membranes have similar negative surface  
239 charge.<sup>48</sup> However, the BW30 membrane has a MWCO of 88 g  $\text{mol}^{-1}$ , hence based on  
240 size exclusion, a much lower uranium penetration into the membrane active layer and  
241 support layer would be expected. In fact, the sorption by TFC-SR2 reached  
242 equilibrium more slowly (generally 30-60 minutes longer) than for BW30, which  
243 would be consistent with slower diffusion of uranium, followed by sorption into the  
244 porous active and support layer structure. The higher sorption onto the TFC-SR2  
245 membrane as opposed to the BW30 membrane could hence be caused by a higher  
246 surface area available for the uranium species to sorb onto the membrane.

247 To provide further evidence for the penetration of uranium into the TFC-SR2  
248 membrane,  $\mu$ -XRF analysis was performed on four selected membrane samples after  
249 experiments at pH 6 and pH 8.5 for both BW30 and TFC-SR2. These pH values were  
250 selected in order to investigate a point of high sorption of uranium at pH 6 and one of  
251 lower uranium sorption at pH 8.5. The  $\mu$ -XRF analysis showed significant differences  
252 with regards to uranium distribution for both membranes studied (Figure 2). As the  
253 spatial resolution of this method is relatively low (the incident X-ray beam size is 10

254  $\mu\text{m}$  and penetrates through the sample so the lateral resolution is very low *i.e.* mm  
255 range), the exact location of uranium cannot be conclusively determined, *i.e.* whether  
256 uranium is present in the active layer, support layer or both, since the NF/RO  
257 membrane active layers have a thickness of around 200 nm.<sup>49</sup> Neither the thickness of  
258 the active layer nor that of the membrane can be accurately determined with this  
259 method as the method picks up the sulfur signal of the polysulphone support layer but  
260 not the signal corresponding to the polyester support layer. However, the sulfur  
261 signals indicate the presence of the polysulfone support layer, whereas the calcium  
262 signals indicate the *approximate* boundaries of the membrane since the calcium  
263 signals originate from the mounting material (see Supporting Information). The XRF  
264 analysis presented in Figure 2 a confirms that uranium entered into the more open  
265 membrane structure of the TFC-SR2 at pH 6, as the uranium peak for this membrane  
266 overlapped with the sulfur peak. In contrast, no uranium could be detected for the  
267 BW30 membrane (Figure 2 c), showing low or no penetration into this membrane.  
268 Size exclusion hence plays an important role in uranium sorption. At pH 8.5, albeit  
269 lower compared to pH 6 due to charge repulsion, uranium penetration and internal  
270 sorption occurred for the TFC-SR2 membrane (Figure 1 and Figure 2 b). This  
271 occurred independently of conditions of charge repulsion between the negatively  
272 charged membrane and the negatively charged uranium species, showing the effect of  
273 membrane pore size and hence size exclusion in uranium penetration and sorption into  
274 the membrane structure. Uranium sorption onto the more opened TFC-SR2 membrane  
275 is hence not only governed by charge interactions but also by access to internal  
276 surface area governed by membrane pore size. In contrast, no uranium could be  
277 detected for the BW30 membrane for pH 8.5, as can be seen in Figure 2 d, showing

278 that any sorption observed in Figure 1 by this membrane was not likely to occur deep  
279 inside the membrane structure but mainly on the surface: uranium sorption for the  
280 dense RO membrane is hence governed by charge interactions. The lower penetration  
281 into BW30 compared to TFC-SR2 hence indicates that membrane pore size acts as a  
282 limiting factor to sorption of uranium by the membranes. Pore size has similarly been  
283 determined as an important factor in membrane sorption of hormones.<sup>50</sup>

284

285 **Uranium sorption by membrane at pressures 5-15 bar.** The previous section  
286 demonstrated the higher penetration of uranium species into the membrane of greater  
287 porosity (TFC-SR2), across the pH range and irrespective of uranium species present.  
288 The objective of these experiments was to investigate the effect of pressure on the  
289 uranium sorption to the membranes. Pressure is likely to enhance the permeation of  
290 solutes inside the membrane and hence facilitate access to the internal membrane  
291 surface area, where sorption may occur. It may also lead to a higher concentration of  
292 uranium at the membrane surface (through concentration polarisation) and, as a  
293 consequence, precipitation might occur. To investigate this, a pressure range of 5-15  
294 bar was selected based on the typical range for spiral wound membranes (3-20 bar)<sup>51</sup>  
295 and manufacturer recommendations.<sup>52,53</sup> Again, pH values 6 and 8.5 were selected.

296

297 The resulting membrane sorption of uranium as a function of pressure is presented in  
298 Figure 3. The sorption varied significantly between membrane types and also between  
299 pH values and thus uranium species present. For TFC-SR2 at pH 6, a constant  
300 sorption of  $50 \pm 5\%$  of uranium (equivalent to a range of 109-125 mg U m<sup>-2</sup> of the  
301 membrane surface) was observed across the pressure range (5-12.5 bar) (Figure 3a);

302 only at 15 bar was there a significant increase in uranium sorption to 69%. The  
303 sorption for the same membrane but at pH 8.5 was different: sorption *increased with*  
304 *pressure*, from < 20% at 5 bar up to 61% at 12.5 and 15 bar (Figure 3b). Conversely,  
305 for BW30 the sorption of uranium by the membrane remained unaffected by pressure  
306 at both pH 6 and pH 8.5 (Figure 3c and d). The results show that irrespectively of  
307 pressure and pH, uranium sorption is higher in TRC-SR2 than in BW30. TFC-SR2  
308 also gave lower retention for uranium, across the pressure range of 5-15 bar: 90%  $\pm$   
309 6% at pH 6, 94%  $\pm$  5% at pH 8.5 while for BW30 uranium retention was 99.7%  $\pm$   
310 0.3% for both pH values and across the entire pressure range. The results are  
311 consistent with the larger pore size of TFC-SR2 compared to BW30 which is related  
312 with permeability. The permeability of the two membranes were compared using the  
313 pure water flux before and after completed experiments, and the permeate flux during  
314 experiments (Figure 4). Pure water flux for BW30 was approximately half of that for  
315 TFC-SR2 at the same pressure, reflecting the difference in permeability between the  
316 two membranes. As expected, BW30 experienced a flux decline during the uranium  
317 experiments, consistent with effects of concentration polarisation and osmotic  
318 pressure difference between the feed and permeate side.<sup>54</sup> Once the pure water flux  
319 was again measured after the uranium experiments, it was restored to its original  
320 value. By contrast, the flux of TFC-SR2 unexpectedly increased with the addition of  
321 experimental solution (and also with addition of salt solution not containing uranium;  
322 results not included) and remained high even when the experimental solution was  
323 drained and pure water was filtered. Although unusual, a similar effect has been  
324 reported by several studies.<sup>55-57</sup> Nilsson et al. linked the flux increase to pore  
325 expansion caused by salt ions reducing the strength of the membrane cross-links.<sup>57</sup>



326 Such pore expansion within the TFC-SR2 membrane would further enhance the  
327 penetration of uranium into the membrane.

328

329 Furthermore, concentration polarisation, which increases with increasing  
330 permeability, is likely to affect the filtration, leading to an accumulation of solutes  
331 and consequently higher concentration adjacent to the membrane surface. Taking  
332 concentration polarisation into account, the solute concentration at the membrane  
333 surface was calculated using Equation 2,<sup>44</sup>

334

$$\frac{C_m - C_p}{C_b - C_p} = \exp\left(\frac{J_v}{k}\right) \quad \text{Eq. 2}$$

337

338 where  $C_m$  = concentration at membrane surface ( $\text{mg L}^{-1}$ ),  $C_p$  = concentration in  
339 permeate ( $\text{mg L}^{-1}$ ),  $C_b$  = concentration in bulk solution ( $\text{mg L}^{-1}$ ),  $J_v$  = permeate flux  
340 ( $\text{m s}^{-1}$ ) and  $k$  = the mass transfer coefficient ( $\text{m s}^{-1}$ ). Whereas  $C_p$ ,  $C_b$  and  $J_v$  are  
341 determined experimentally,  $k$  had to be calculated using correlations relevant to the  
342 experimental conditions (slit channel and laminar flow). For the experimental  
343 conditions of the system used, the Sherwood number can be related to the Reynolds  
344 and Schmidt number<sup>58</sup> as described in Equation 3:

345

$$Sh = 1.85 \times Re^{0.33} Sc^{0.33} (d_h / L)^{0.33} \quad \text{Eq. 3}$$

346

348 where  $Re$  = the Reynolds number,  $Sc$  = the Schmidt number,  $dh$  = channel hydraulic  
349 diameter,  $L$  = the length of the membrane cell. The Reynolds, Schmidt and Sherwood  
350 number were calculated as described in Semião et al.<sup>37</sup>

351

352 The extent of concentration polarisation experienced by a membrane can be reported  
353 as the concentration polarisation modulus, giving the ratio of initial concentration at  
354 the membrane surface ( $C_m$ ) to that in the bulk solution ( $C_b$ ) at the start of the  
355 experiment. The concentration polarisation modulus for each pressure experiment are  
356 displayed together with the uranium uptake in Figure 3. During filtration with BW30,  
357 uranium uptake (around 30 and 20% for pH 6 and 8.5, respectively) for both pH  
358 values remained unaffected by pressure and concentration polarisation (Figure 3c and  
359 d). Due to its high permeability the TFC-SR2 membrane was more affected than  
360 BW30 by concentration polarisation. There were some important differences between  
361 the results for TFC-SR2 at the two pH values. At pH 8.5, uranium sorption to the  
362 membrane clearly followed the polarisation modulus trend. This trend was similar to a  
363 previous study with hormones and a NF270 membrane, where higher polarisation  
364 modulus resulted in higher concentration at the membrane surface translating into a  
365 higher adsorption.<sup>37</sup> In contrast, at pH 6 the uranium uptake to the TFC-SR2  
366 membrane remained constant despite pressure and concentration polarisation increase,  
367 with the exception of the highest pressure point. It appears that concentration  
368 polarisation does not affect the interaction between the uranium species and  
369 membrane at pH 6, suggesting that variations in uranium concentration only have a  
370 small effect on the amount of uranium sorbed by the membranes. To confirm this, an  
371 adsorption isotherm for uranium at pH 6 was plotted (Figure S2). Using linear fit of

372 the sorption isotherm, the uranium sorption, based on the concentration at the  
373 membrane surface  $C_m$  of 0.62-1.03 mg L<sup>-1</sup> for pressures 5 to 15, was estimated to  
374 around 107-123 mg U m<sup>-2</sup> of membrane surface, i.e. a sorption of 50% to 57% based  
375 on mass balance, showing that pressure and hence concentration polarisation had an  
376 insignificant effect on uranium sorption at pH 6. Precipitation as an uptake  
377 mechanism could be excluded, as even at high concentration polarisation the uranium  
378 concentration at the membrane surface was calculated to be a maximum of 1.03 mg L<sup>-1</sup>  
379 and still remained below maximum solubility of uranium, thus confirming sorption  
380 to be the main mechanism governing uranium-membrane interactions.

381

382 This study confirmed that the uranium-membrane interactions were highly speciation  
383 and pH dependent, with affinity determined by the charge of both membrane and  
384 uranium species (*e.g.* UO<sub>2</sub>OH<sup>+</sup> or UO<sub>2</sub>(CO<sub>3</sub>)<sub>3</sub><sup>4-</sup>) as well as species size relative to  
385 membrane pore size. Pore size and subsequent permeability of the membranes  
386 governed uranium sorption, where TFC-SR2 was subject to higher uranium sorption  
387 than BW30 under all experimental conditions. Concentration polarisation affected  
388 only one of the uranium species, UO<sub>2</sub>(CO<sub>3</sub>)<sub>3</sub><sup>4-</sup>, a species which generally tends to  
389 display low sorption and high mobility,<sup>59,60</sup> but its sorption to TFC-SR2 increased  
390 with increasing pressure. UO<sub>2</sub>OH<sup>+</sup>, whose sorption to TFC-SR2 was initially higher,  
391 remained largely unaffected by concentration polarisation. This study has provided a  
392 first insight into the nature of the interactions of uranium with NF and RO membranes  
393 and the clear effects of pH and charge interactions, membrane pore size and  
394 concentration polarisation on uranium sorption. Uranium sorption might be further  
395 affected by the presence of different functional groups on the membrane active layer.

396 Tang et al,<sup>61</sup> for example, showed that some RO membranes possess a surface layer  
397 coating rich in -COH groups in addition to the aromatic or semi-aromatic polyamide  
398 active layer. Hence, future work focused on a more in-depth analysis to determine the  
399 chemical nature and spatial distribution of the uranium sorption to the membranes, as  
400 well as the effect of hardness on the removal of uranium by NF and RO membranes is  
401 needed.

402

403 The results are of significance in the wider membrane application context since it  
404 illustrates the importance of taking sorption of contaminants into account. The  
405 retention *observed* in experimental and applied water treatment settings may not be  
406 the actual or real retention, and the long-term consequences of sorption to the  
407 membranes remains unknown. One possible consequence is the risk of uranium de-  
408 sorption from the membrane into the permeate line during operation, especially at  
409 acidic pH values, which could pose a health risk to water consumers. There is great  
410 variability in membrane life-time and performance from location to location and  
411 contaminant sorption (not necessarily picked up since it may not cause obvious  
412 fouling and consequent flux decline) may be one of the determining factors.

413

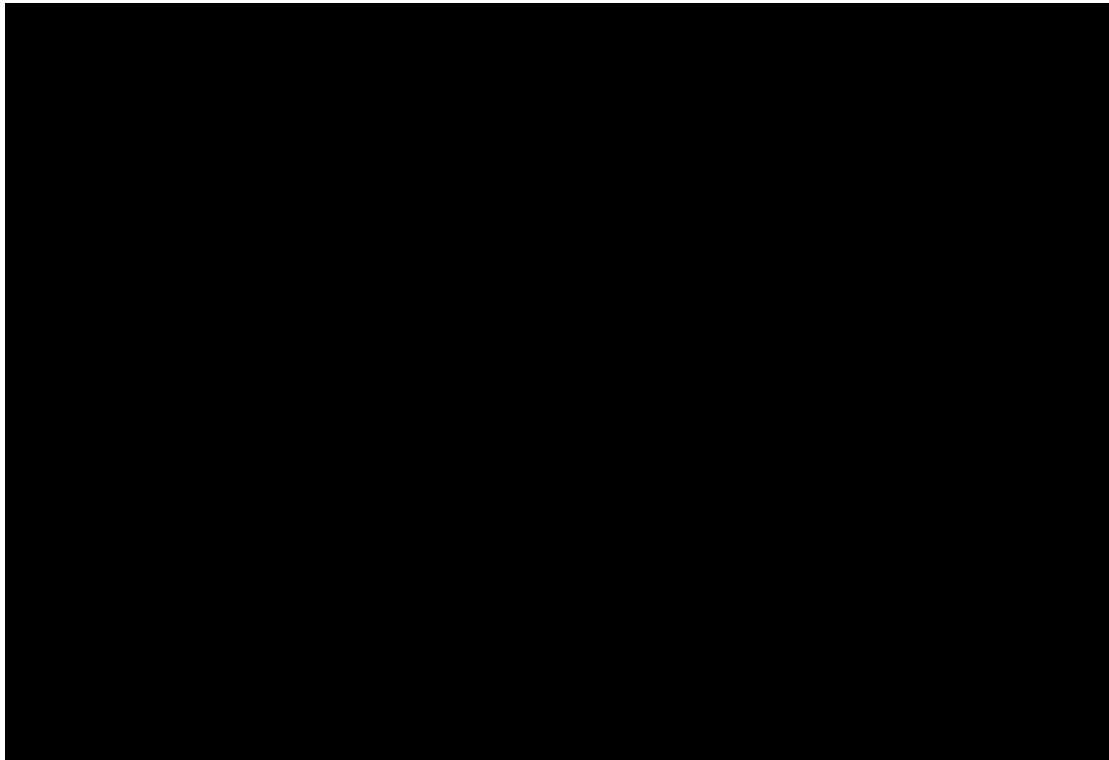
414

415

416

417 FIGURES

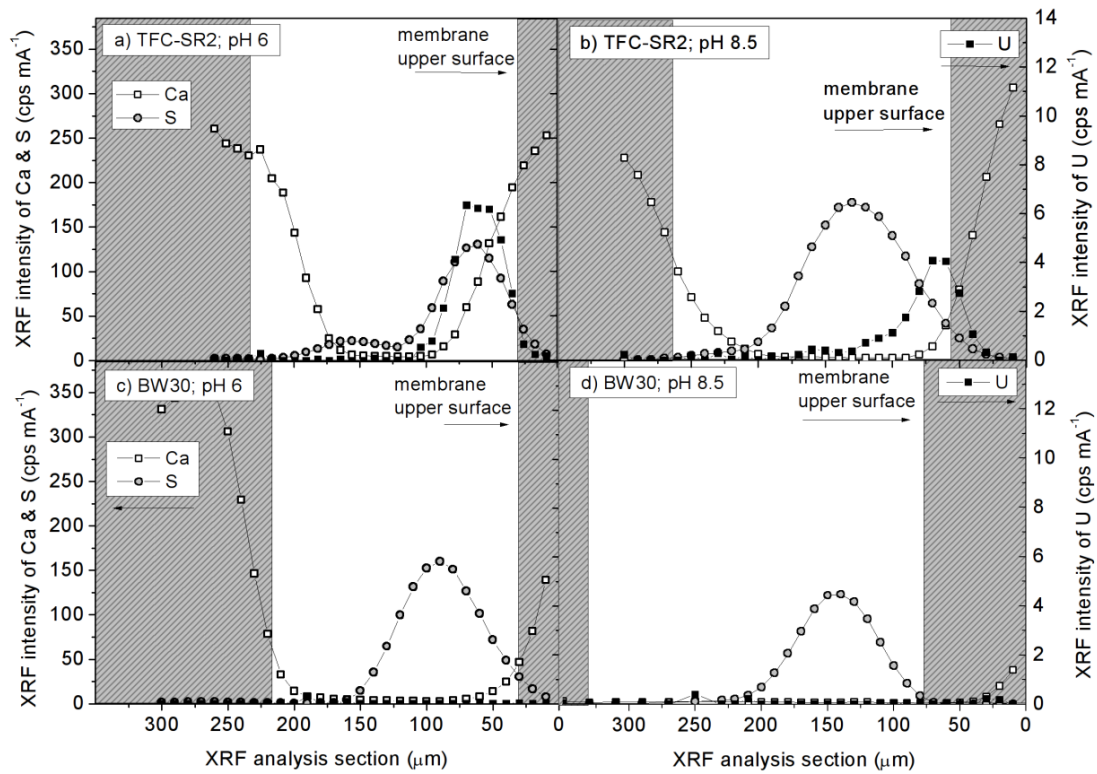
418



419

420 Figure 1. Uranium speciation (lines) and uranium uptake or sorption (columns)  
421 by membranes TFC-SR2 and BW30 across the pH range 3-10. Experimental  
422 solution: 0.5 mg L<sup>-1</sup> uranium, 20 mM NaCl and 1 mM NaHCO<sub>3</sub>. Experimental  
423 conditions: flow-rate = 0.6 L min<sup>-1</sup>, temperature = 24°C, no applied pressure.  
424 The variation in uptake was within ± 4% for repeated experiments for TFC-  
425 SR2 and ± 1% for BW30.

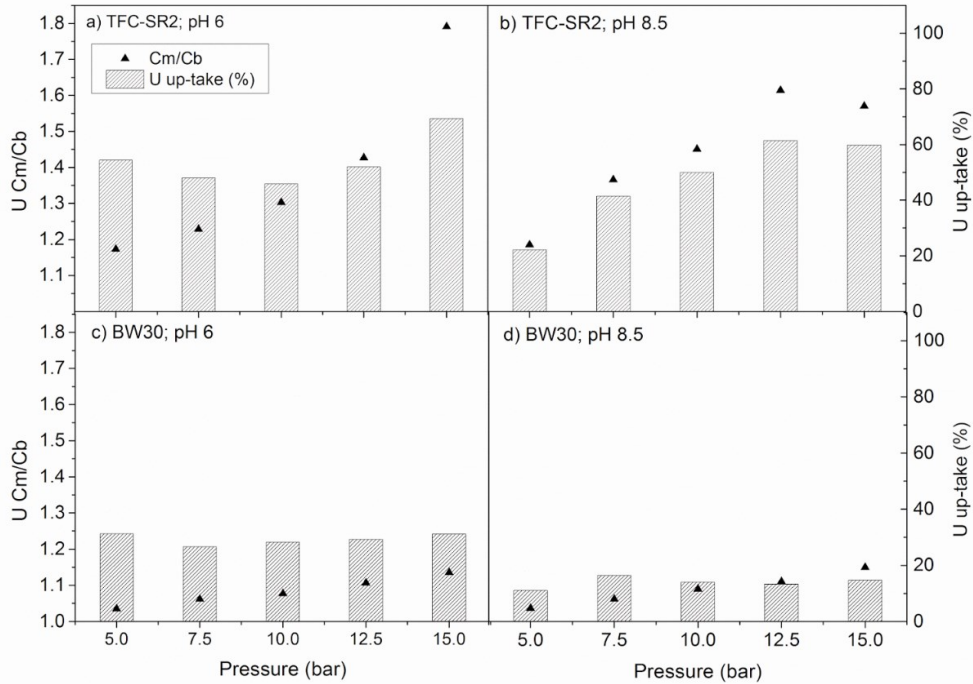
426



427

428 Figure 2. Cross-sections of TFC-SR2 and BW30 showing the elemental  
 429 distribution of U, S and Ca for experiments performed without pressure for  
 430 TFC-SR2 at pH 6 (a) and pH 8.5 (b) and BW30 at pH 6 (c) and pH 8.5 (d)  
 431 determined by  $\mu$ -XRF. The *approximate* top and bottom edge of the  
 432 membrane is indicated by the shaded area based on the detection of the  
 433 calcium mounting material. Note the different intensity scales for Ca and S  
 434 compared to U.

435

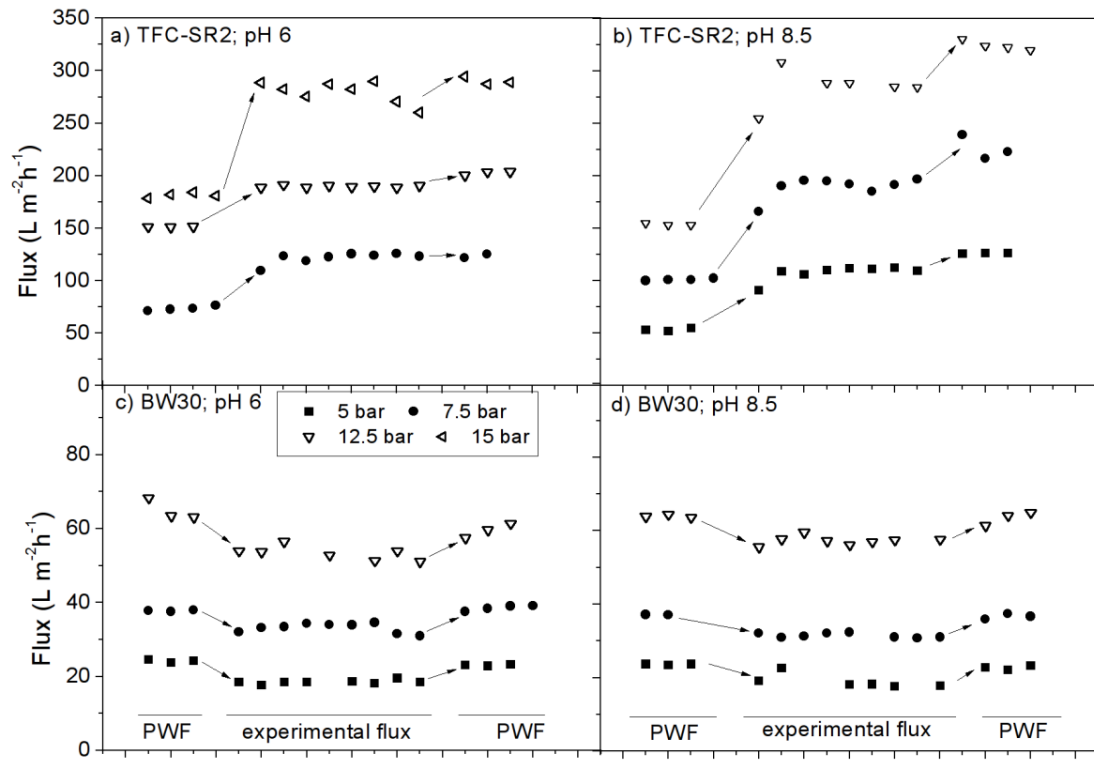


436

437 Figure 3. The percentage uptake (sorption) of uranium (columns) during the  
 438 experiments is shown on the right y-axis, while the calculated polarisation  
 439 modulus ( $C_m/C_b$ ) for uranium is indicated by points and displayed on the left  
 440 y-axis. Repeatability of U uptake for selected experiments was within  $\pm 4\%$  for  
 441 TFC-SR2 and  $\pm 1\%$  for BW30.

442

443





445 Figure 4. Pure water flux (PWF) before and after selected pressure  
 446 experiments, and permeate flux during pressure experiments (5-15 bar) for  
 447 TFC-SR2 and BW30 at pH 6 and 8.5. Permeability variability for TFC-SR2  
 448 was  $\pm 13\%$  and BW30 was  $\pm 3\%$  based on pure water flux experiments.  
 449 Variability of permeate flux during experiments was within  $\pm 10\%$  for TFC-SR2  
 450 and  $\pm 2\%$  for the BW30. Please note different flux scales for TFC-SR2 and  
 451 BW30.

452

453 TABLES

454 Table 1. Membrane characteristics

Parameter	TFC-SR2	BW30
Iso-electric point/pH	4.25	4.19
Nominal MWCO/g mol <sup>-1</sup>	486 <sup>a</sup>	88
Pore radius/nm	0.52 $\pm$ 0.03	0.32 $\pm$ 0.01 <sup>b,43</sup>
Permeability/L m <sup>-2</sup> h <sup>-1</sup> bar <sup>-1</sup>	10.97 $\pm$ 1.51	4.84 $\pm$ 0.15

455 <sup>a</sup>Absolute MWCO (100% retention) for TFC-SR2 was determined as 1033 g mol<sup>-1</sup>.

456 <sup>b</sup>Note that RO membranes are considered to have dense, non-porous structures and so  
 457 “pore-radius” for BW30 was determined only as a comparison with the more open  
 458 structure of TFC-SR2.

459

460

461 Table 2. Main uranium species present for pH range 3-10<sup>a</sup>

pH value	Uranium species	Molecular weight (g mol <sup>-1</sup> )
3-4	UO <sub>2</sub> <sup>2+</sup>	270
5-6	UO <sub>2</sub> OH <sup>+</sup>	287

6-7	$\text{UO}_2\text{CO}_3$	330
7	$(\text{UO}_2)_2\text{CO}_3(\text{OH})_3^-$	651
8	$\text{UO}_2(\text{CO}_3)_2^{2-}$	390
8-10	$\text{UO}_2(\text{CO}_3)_3^{4-}$	450

462 <sup>a</sup>Note that each pH value may contain a mixture of several species.

463

464

465

466 ASSOCIATED CONTENT

467 **Supporting information.** Details of experimental set-up and filtration procedure,  
 468 ICP-OES, ICP-MS and XRF analysis, salt retention and isotherm experiment. This  
 469 material is available free of charge via the internet at <http://pubs.acs.org>.

470

471 AUTHOR INFORMATION

472 **Corresponding Author**

473 \*Tel +46 (0)87906291

474 E-mail: [hschulte@kth.se](mailto:hschulte@kth.se)

475

476 **Present Addresses**

477 \*Department for Sustainable Development, Environmental Science and Engineering  
 478 (SEED), KTH Royal Institute of Technology, Teknikringen 76 1 tr, SE-100 44  
 479 Stockholm, Sweden.

480

481 **Author Contributions**

482 The manuscript was written through contributions of all authors. All authors have  
483 given approval to the final version of the manuscript.

484

#### 485 **Funding Sources**

486 ESRC-EPSRC PhD scholarship, FFWG for additional living allowance and EPSRC  
487 Doctoral Prize Fellowship for H. Schulte-Herbrüggen.

488

#### 489 ACKNOWLEDGMENT

490 **Acknowledgements.** The authors are grateful to the following organisations and  
491 individuals: The School of Engineering (University of Edinburgh, UoE) for funding  
492 cross-flow equipment, Koch Membrane Systems and Filmtec Corporation for NF and  
493 RO membrane sheets, Dr Annalisa De-Munari (UoE), Dr Alexander Bismarck and Dr  
494 Kingsley Ho (Imperial College, UK) for zeta potential measurements, Steven Gourlay  
495 (UoE) for cross-flow system design, Dr Alan Simm (UoE) for LabVIEW set up, Dr  
496 Lorna Eades (UoE) for assistance with ICP-MS analysis. Prof Andrea Schäfer (UoE)  
497 is thanked for facilitating the work and Prof Viatcheslav Freger (Technion, Israel) and  
498 the anonymous reviewers are thanked for constructive suggestions to improve the  
499 work.

500

#### 501 References.

- 502 (1) Wada, Y.; van Beek, L. P. H.; van Kempen, C. M.; Reckman, J. W. T. M.;  
503 Vasak, S.; Bierkens, M. F. P. Global depletion of groundwater resources.  
504 *Geophys. Res. Lett.* **2010**, *37* (20), L20402.  
505 (2) MacDonald, A. M.; Bonsor, H. C.; Dochartaigh, B. É. Ó.; Taylor, R. G.  
506 Quantitative maps of groundwater resources in Africa. *Environ. Res. Lett.* **2012**,  
507 *7* (2), 24009.

- 508 (3) Estrela, T.; Marcuello, C.; Iglesias, A. *Water resources problems in Southern*  
509 *Europe*; 1996.
- 510 (4) Nriagu, J.; Nam, D.-H.; Ayanwola, T. A.; Dinh, H.; Erdenechimeg, E.; Ochir,  
511 C.; Bolormaa, T.-A. High levels of uranium in groundwater of Ulaanbaatar,  
512 Mongolia. *Sci. Total Environ.* **2012**, *414*, 722–726.
- 513 (5) Norrström, A. C.; Löf, Å. Uranium theoretical speciation for drinking water  
514 from private drilled wells in Sweden – Implications for choice of removal  
515 method. *Appl. Geochem.* **2014**, *51*, 148–154.
- 516 (6) Vesterbacka, P. Natural radioactivity in drinking water in private wells in  
517 Finland. *Radiat. Prot. Dosimetry* **2004**, *113* (2), 223–232.
- 518 (7) Winde, F.; Jacobus van der Walt, I. The significance of groundwater–stream  
519 interactions and fluctuating stream chemistry on waterborne uranium  
520 contamination of streams—a case study from a gold mining site in South Africa.  
521 *J. Hydrol.* **2004**, *287* (1–4), 178–196.
- 522 (8) Arogunjo, A. M.; Höllriegl, V.; Giussani, A.; Leopold, K.; Gerstmann, U.;  
523 Veronese, I.; Oeh, U. Uranium and thorium in soils, mineral sands, water and  
524 food samples in a tin mining area in Nigeria with elevated activity. *J. Environ.*  
525 *Radioact.* **2009**, *100* (3), 232–240.
- 526 (9) Vandenhove, H.; Sweeck, L.; Mallants, D.; Vanmarcke, H.; Aitkulov, A.;  
527 Sadyrov, O.; Savosin, M.; Tolongutov, B.; Mirzachev, M.; Clerc, J. J.; et al.  
528 Assessment of radiation exposure in the uranium mining and milling area of  
529 Mailuu Suu, Kyrgyzstan. *J. Environ. Radioact.* **2006**, *88* (2), 118–139.
- 530 (10) Vandenhove. European sites contaminated by residues from the ore-  
531 extracting and -processing industries. *Int. Congr. Ser.* **2002**, *1225*, 307–325.
- 532 (11) Craft, E. S.; Abu-Qare, A. W.; Flaherty, M. M.; Garofolo, M. C.; Rincavage, H.  
533 L.; Abou-Donia, M. B. Depleted and natural uranium: chemistry and  
534 toxicological effects. *J. Toxicol. Environ. Health Part B* **2004**, *7* (4), 297–317.
- 535 (12) Kurttio, P.; Harmoinen, A.; Saha, H.; Salonen, L.; Karpas, Z.; Komulainen, H.;  
536 Auvinen, A. Kidney Toxicity of Ingested Uranium From Drinking Water. *Am. J.*  
537 *Kidney Dis.* **2006**, *47* (6), 972–982.
- 538 (13) Prat, O.; Vercouter, T.; Ansoborlo, E.; Fichet, P.; Perret, P.; Kurttio, P.; Salonen,  
539 L. Uranium speciation in drinking water from drilled wells in southern Finland  
540 and its potential links to health effects. *Environ. Sci. Technol.* **2009**, *43* (10),  
541 3941–3946.
- 542 (14) Vicente-Vicente, L.; Quiros, Y.; Perez-Barriocanal, F.; Lopez-Novoa, J. M.;  
543 Lopez-Hernandez, F. J.; Morales, A. I. Nephrotoxicity of Uranium:  
544 Pathophysiological, Diagnostic and Therapeutic Perspectives. *Toxicol. Sci.* **2010**,  
545 *118* (2), 324–347.
- 546 (15) Miller, A. C.; Brooks, K.; Smith, J.; Page, N. Effect of the militarily-relevant  
547 heavy metals, depleted uranium and heavy metal tungsten-alloy on gene  
548 expression in human liver carcinoma cells (HepG2). *Mol. Cell. Biochem.* **2004**,  
549 *255* (1–2), 247–256.
- 550 (16) Hogan, A.; Vandam, R.; Markich, S.; Camilleri, C. Chronic toxicity of uranium  
551 to a tropical green alga ( sp.) in natural waters and the influence of dissolved  
552 organic carbon. *Aquat. Toxicol.* **2005**, *75* (4), 343–353.
- 553 (17) Kurttio, P.; Auvinen, A.; Salonen, L.; Saha, H.; Pekkanen, J.; Mäkeläinen, I.;  
554 Väisänen, S. B.; Penttilä, I. M.; Komulainen, H. Renal effects of uranium in  
555 drinking water. *Environ. Health Perspect.* **2002**, *110* (4), 337.

- 556 (18) Kurttio, P.; Komulainen, H.; Leino, A.; Salonen, L.; Auvinen, A.; Saha, H. Bone  
557 as a Possible Target of Chemical Toxicity of Natural Uranium in Drinking  
558 Water. *Environ. Health Perspect.* **2004**, *113* (1), 68–72.
- 559 (19) World Health Organization. *Guidelines for drinking-water quality*; World  
560 Health Organization: Geneva, 2011.
- 561 (20) Birke, M.; Rauch, U.; Lorenz, H.; Kringel, R. Distribution of uranium in German  
562 bottled and tap water. *J. Geochem. Explor.* **2010**, *107* (3), 272–282.
- 563 (21) Cyna, B.; Chagneau, G.; Bablon, G.; Tanghe, N. Two years of nanofiltration at  
564 the Méry-sur-Oise plant, France. *Desalination* **2002**, *147* (1–3), 69–75.
- 565 (22) Service, R. F. Desalination Freshens Up. *Science* **2006**, *313* (5790), 1088–1090.
- 566 (23) Al-Amoudi, A.; Lovitt, R. W. Fouling strategies and the cleaning system of NF  
567 membranes and factors affecting cleaning efficiency. *J. Membr. Sci.* **2007**, *303*  
568 (1–2), 4–28.
- 569 (24) Van der Bruggen, B.; Vandecasteele, C. Removal of pollutants from surface  
570 water and groundwater by nanofiltration: overview of possible applications in  
571 the drinking water industry. *Environ. Pollut.* **2003**, *122* (3), 435–445.
- 572 (25) Annamäki, M.; STUK Radiation and Nuclear Safety Authority. *Treatment*  
573 *techniques for removing natural radionuclides from drinking water. Final report*  
574 *of the TENAWA project*; 2000.
- 575 (26) Thomson, M.; Infield, D. A photovoltaic-powered seawater reverse-osmosis  
576 system without batteries. *Desalination* **2003**, *153* (1–3), 1–8.
- 577 (27) Coffey, M. Renewable energy: Filtration and the green energy revolution. *Filtr.*  
578 *Sep.* **2008**, *45* (5), 24–27.
- 579 (28) De Munari, A.; Schäfer, A. I. Membrane plants for drinking water provision in  
580 remote scottish communities: performance, costs and lessons learnt. In  
581 *Membranes in Drinking and Industrial Water*; Trondheim, Norway, 2010.
- 582 (29) Rossiter, H. M. A.; Graham, M. C.; Schäfer, A. I. Impact of speciation on  
583 behaviour of uranium in a solar powered membrane system for treatment of  
584 brackish groundwater. *Sep. Purif. Technol.* **2010**, *71* (1), 89–96.
- 585 (30) Kantar, C. Heterogeneous processes affecting metal ion transport in the presence  
586 of organic ligands: Reactive transport modeling. *Earth-Sci. Rev.* **2007**, *81* (3–4),  
587 175–198.
- 588 (31) Semião, A. J. C.; Rossiter, H. M. A.; Schäfer, A. I. Impact of organic matter and  
589 speciation on the behaviour of uranium in submerged ultrafiltration. *J. Membr.*  
590 *Sci.* **2010**, *348* (1–2), 174–180.
- 591 (32) Langmuir, D. *Aqueous Environmental Geochemistry*; Prentice-Hall, Inc.: Upper  
592 Saddle River, New Jersey, 1997.
- 593 (33) Huikuri, P.; Salonen, L.; Raff, O. Removal of natural radionuclides from  
594 drinking water by point of entry reverse osmosis. *Desalination* **1998**, *119* (1),  
595 235–239.
- 596 (34) Raff, O.; Wilken, R.-D. Removal of dissolved uranium by nanofiltration.  
597 *Desalination* **1999**, *122* (2), 147–150.
- 598 (35) Favre-Reguillon, A.; Lebizit, G.; Foos, J.; Guy, A.; Draye, M.; Lemaire, M.  
599 Selective Concentration of Uranium from Seawater by Nanofiltration. *Ind. Eng.*  
600 *Chem. Res.* **2003**, *42* (23), 5900–5904.
- 601 (36) Favre-Réguillon, A.; Lebizit, G.; Murat, D.; Foos, J.; Mansour, C.; Draye, M.  
602 Selective removal of dissolved uranium in drinking water by nanofiltration.  
603 *Water Res.* **2008**, *42* (4–5), 1160–1166.

- 604 (37) Orloff, K. G.; Mistry, K.; Charp, P.; Metcalf, S.; Marino, R.; Shelly, T.; Melaro,  
605 E.; Donohoe, A. M.; Jones, R. L. Human exposure to uranium in groundwater.  
606 *Environ. Res.* **2004**, *94* (3), 319–326.
- 607 (38) Seldén, A. I.; Lundholm, C.; Edlund, B.; Högdahl, C.; Ek, B.-M.; Bergström, B.  
608 E.; Ohlson, C.-G. Nephrotoxicity of uranium in drinking water from private  
609 drilled wells. *Environ. Res.* **2009**, *109* (4), 486–494.
- 610 (39) Semião, A. J. C.; Schäfer, A. I. Estrogenic micropollutant adsorption dynamics  
611 onto nanofiltration membranes. *J. Membr. Sci.* **2011**, *381* (1–2), 132–141.
- 612 (40) Tang, C. Y.; Kwon, Y.-N.; Leckie, J. O. Effect of membrane chemistry and  
613 coating layer on physiochemical properties of thin film composite polyamide RO  
614 and NF membranes: I. FTIR and XPS characterization of polyamide and coating  
615 layer chemistry. *Desalination* **2009**, *242* (1–3), 149–167.
- 616 (41) Tang, C.; Kwon, Y.; Leckie, J. Probing the nano- and micro-scales of reverse  
617 osmosis membranes—A comprehensive characterization of physiochemical  
618 properties of uncoated and coated membranes by XPS, TEM, ATR-FTIR, and  
619 streaming potential measurements. *J. Membr. Sci.* **2007**, *287* (1), 146–156.
- 620 (42) Hilal, N.; Al-Abri, M.; Al-Hinai, H. Characterization and retention of UF  
621 membranes using PEG, HS and polyelectrolytes. *Desalination* **2007**, *206* (1–3),  
622 568–578.
- 623 (43) Nghiem, L. D.; Schäfer, A. I.; Elimelech, M. Removal of Natural Hormones by  
624 Nanofiltration Membranes: Measurement, Modeling, and Mechanisms. *Environ.*  
625 *Sci. Technol.* **2004**, *38* (6), 1888–1896.
- 626 (44) Sutzkover, I.; Hasson, D.; Semiat, R. Simple technique for measuring the  
627 concentration polarization level in a reverse osmosis system. *Desalination* **2000**,  
628 *131* (1), 117–127.
- 629 (45) Gekas, V.; Hallström, B. Mass transfer in the membrane concentration  
630 polarization layer under turbulent cross flow: I. Critical literature review and  
631 adaptation of existing Sherwood correlations to membrane operations. *J. Membr.*  
632 *Sci.* **1987**, *30* (2), 153–170.
- 633 (46) van den Berg, G. B.; Rácz, I. G.; Smolders, C. A. Mass transfer coefficients in  
634 cross-flow ultrafiltration. *J. Membr. Sci.* **1989**, *47* (1–2), 25–51.
- 635 (47) Borrini, J.; Bernier, G.; Pellet-Rostaing, S.; Favre-Reguillon, A.; Lemaire, M.  
636 Separation of lanthanides(III) by inorganic nanofiltration membranes using a  
637 water soluble complexing agent. *J. Membr. Sci.* **2010**, *348* (1–2), 41–46.
- 638 (48) Negaresh, E.; Antony, A.; Bassandeh, M.; Richardson, D. E.; Leslie, G.  
639 Selective separation of contaminants from paper mill effluent using  
640 nanofiltration. *Chem. Eng. Res. Des.* **2012**, *90* (4), 576–583.
- 641 (49) Freger, V. Swelling and Morphology of the Skin Layer of Polyamide Composite  
642 Membranes: An Atomic Force Microscopy Study. *Environ. Sci. Technol.* **2004**,  
643 *38* (11), 3168–3175.
- 644 (50) Semião, A. J. C.; Schäfer, A. I. Removal of adsorbing estrogenic micropollutants  
645 by nanofiltration membranes. Part A—Experimental evidence. *J. Membr. Sci.*  
646 **2013**, *431*, 244–256.
- 647 (51) Thorsen, T.; Fløgstad, H. *Nanofiltration in drinking water treatment*; Literature  
648 review D5. 3. 4B; Techneau, 2006.
- 649 (52) Dow Filmtec. Dow Filmtec Membranes.
- 650 (53) Koch Membrane Systems. Fluid Systems TFC-SR2 2.5" Element.

- 651 (54) Sablani, S.; Goosen, M.; Al-Belushi, R.; Wilf, M. Concentration polarization in  
652 ultrafiltration and reverse osmosis: a critical review. *Desalination* **2001**, *141* (3),  
653 269–289.
- 654 (55) Wang, Y.; Shu, L.; Jegatheesan, V.; Gao, B. Removal and adsorption of diuron  
655 through nanofiltration membrane: The effects of ionic environment and  
656 operating pressures. *Sep. Purif. Technol.* **2010**, *74* (2), 236–241.
- 657 (56) De Munari, A.; Schäfer, A. I. Impact of speciation on removal of manganese and  
658 organic matter by nanofiltration. *J. Water Supply Res. Technol.* **2010**, *59* (2–3),  
659 152.
- 660 (57) Nilsson, M.; Trägårdh, G.; Östergren, K. The influence of sodium chloride on  
661 mass transfer in a polyamide nanofiltration membrane at elevated temperatures.  
662 *J. Membr. Sci.* **2006**, *280* (1–2), 928–936.
- 663 (58) Schock, G.; Miquel, A. Mass transfer and pressure loss in spiral wound modules.  
664 *Desalination* **1987**, *64*, 339–352.
- 665 (59) Wazne, M.; Meng, X.; Korfiatis, G. P.; Christodoulatos, C. Carbonate effects on  
666 hexavalent uranium removal from water by nanocrystalline titanium dioxide. *J.*  
667 *Hazard. Mater.* **2006**, *136* (1), 47–52.
- 668 (60) Maher, K.; Bargar, J. R.; Brown, G. E. Environmental Speciation of Actinides.  
669 *Inorg. Chem.* **2013**, *52* (7), 3510–3532.
- 670 (61) Tang, C. Y.; Kwon, Y.-N.; Leckie, J. O. Effect of membrane chemistry and  
671 coating layer on physiochemical properties of thin film composite polyamide RO  
672 and NF membranes. *Desalination* **2009**, *242* (1–3), 168–182.  
673